Marine *Synechococcus* Picocyanobacteria: Light Utilization Across Latitudes

Christophe Six, Morgane Ratin, Dominique Marie & Erwan Corre.

Corresponding author: C. Six, six@sb-roscoff.fr

SUPPLEMENTARY INFORMATION

Table of content:

SUPPLEMENTARY MATERIAL

Section 1: Thermal photophysiology of marine *Synechococcus*

Table S1: Information regarding the marine *Synechococcus* strains used in this study. The phylogenetic position has been shown in several studies including (1–4). The pigment types were defined in (5, 6). **PEB**, phycoerythrobilin; **PUB**, phycourobilin; **CA**, chromatic adapter.

Strain name	RCC #	Isolation latitude	Isolation longitude	Isolation site	Phylogenetic position	Phycobilisome pigment type	Ecotype
M16.1	791	+27.70	-91.30	Gulf of Mexico	Clade IIa	3a (PEB-rich)	Tropical
RS9907	2382	+29.47	+34.92	Gulf of Aqaba	Clade IIa	3a (PEB-rich)	Tropical
A15-44	2527	+21.68	+17.83	Sahara coast	Clade IIa	2 (PEB)	Tropical
WH7803	752	+33.75	-67.50	Sargasso Sea	Clade V	3a (PEB-rich)	Coastal tropical
RS9915	2553	+ 29.47	+34.92	Gulf of Aqaba	Clade IIIa	3d (CA)	Warm-temperate
WH8102	539	+22.48	-65.60	Caribbean Sea	Clade IIIa	3c (PUB-rich)	Warm-temperate
BOUM118	2421	+33.63	+32.63	East Med Sea	Clade IIIa	3c (PUB-rich)	Warm-temperate
BL107	515	+41.72	+3.55	Balearic Sea	Clade IVa	3d (CA)	Cold temperate
MVIR-16-1	2570	+60.32	-3.48	North Sea	Clade IVa	3d (CA)	Cold temperate
MVIR-18-1	2385	+61.00	+1.98	Norway Sea	Clade Ib	3a (PEB-rich)	Coastal subpolar
SYN20	2035	+60.27	+5.20	Norway Sea	Clade Ib	3a (PEB-rich)	Coastal subpolar
WH8016	2535	+41.52	-70.67	Buzzards Bay	Clade Ib	3a (PEB-rich)	Coastal subpolar

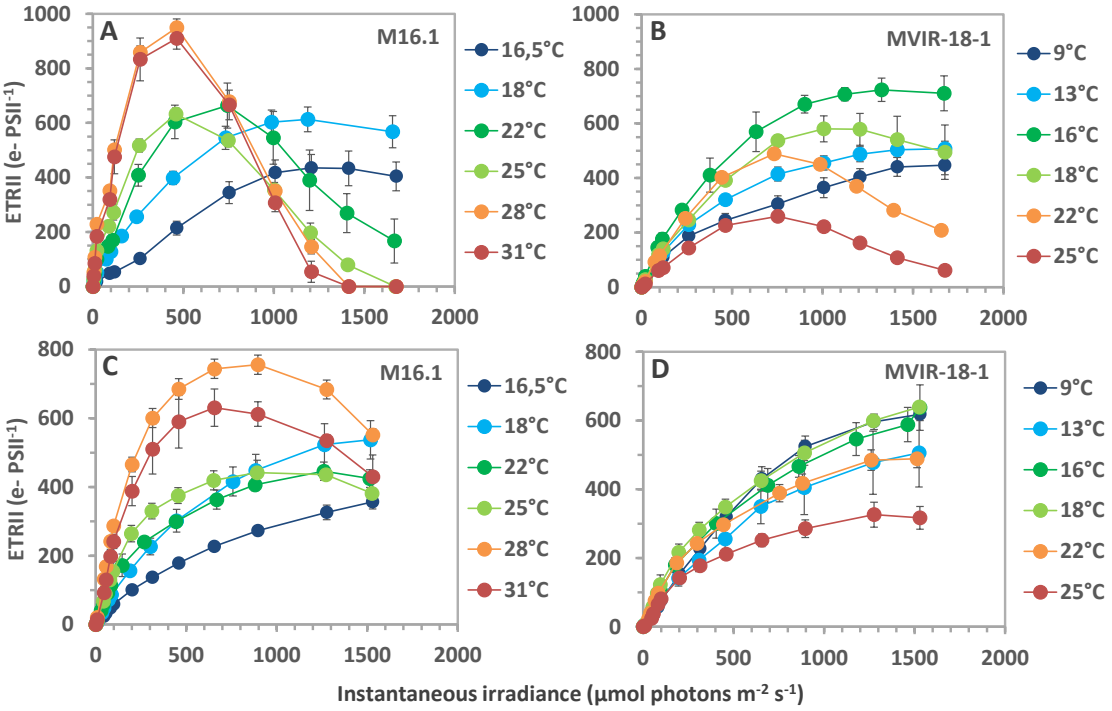

Figure S1: Photosystem II electron transport versus irradiance (photosynthesis / Energy; P/E) curves recorded by pulse amplitude modulation fluorometry. The initial slope α and the saturation irradiance E_K were retrieved by fitting the Platt model (7). Curves recorded at 540 nm for *Synechococcus* spp. M16.1 (**A**) and MVIR-18-1 (**B**) at different growth temperatures. Curves recorded at 480 nm for *Synechococcus* spp. M16.1 (**C**) and MVIR-18-1 (**D**) at different growth temperatures.

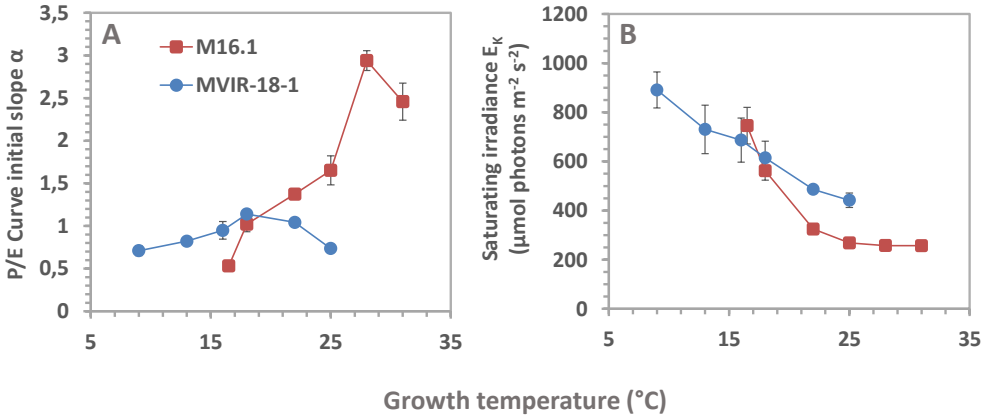

Figure S2: Variations of the initial curve slope α (**A**) and the saturation irradiance (**B**) using 480 nm light, in Synechococcus spp. M16.1 (red) and MVIR-18-1 (blue).

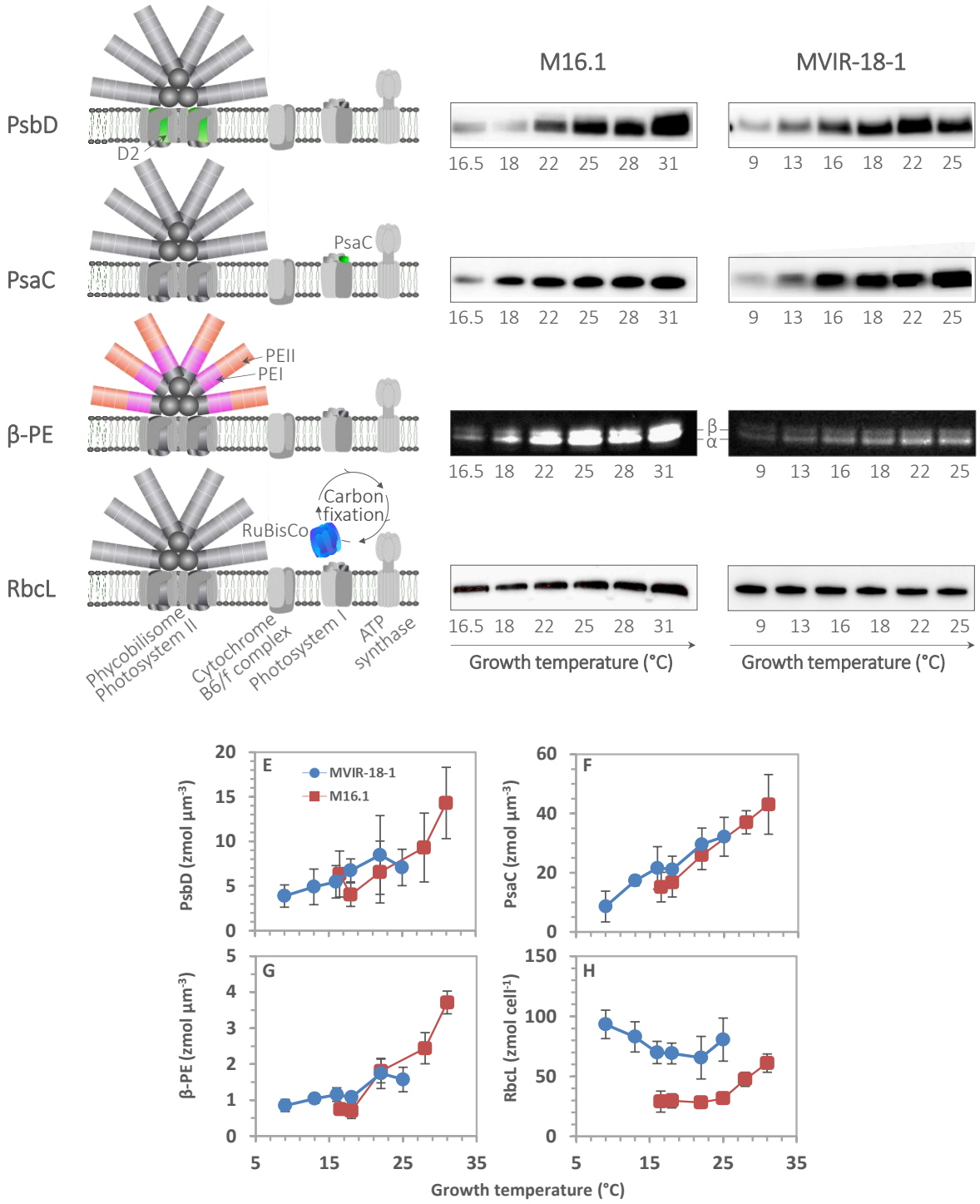

Figure S3: In-gel fluorescence photo (**A**), immunoblots (**B**, **C**, **D**) and quantified variations of the proteins targeted to represent the major photosynthetic complexes in *Synechococcus* spp. M16.1 and MVIR-18-1, function of growth temperature. **A**: Both phycoerythrins I and II could be quantified by fluorescence using their β-PE subunits CpeB and MpeB, respectively, which have the same optical properties in the *Synechococcus* pigment type 3a (5, 8). **B**: Reaction centers II were quantified using the major core protein PsbD (D2). **C**: Reaction centers I were quantified using the small Fe-S binding protein PsaC. **D**: The Ribulose 1,5-bis phosphate Carboxylase Oxygenase (RuBisCO), catalyzing carbon fixation in the Calvin-Benson cycle, was quantified using its large subunit RbcL. Simplified diagrams illustrate the location of these proteins in the different protein complexes. **E**: Phycoerythrin β-subunits variations expressed in zmol per µm^3 cell. **F**: PsbD variations expressed in zmol per µm^3 cell. **G**: PsaC variations expressed in zmol per µm^3 cell. **H**: RbcL variations expressed in zmol per cell.

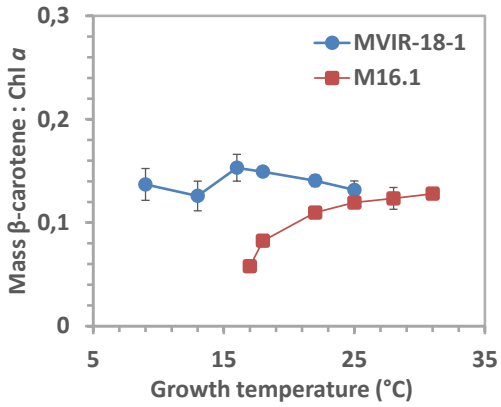

Figure S4: Variations in the mass ratio β-carotene to chlorophyll a in *Synnechococcus* spp. MA6.1 (red) and MVIR-18-1 (blue) grown over their thermal *preferendum*, as measured by high pressure liquid chromatography. The cultures were grown under 80 µmol photons m^{-2} s^{-1} white light.

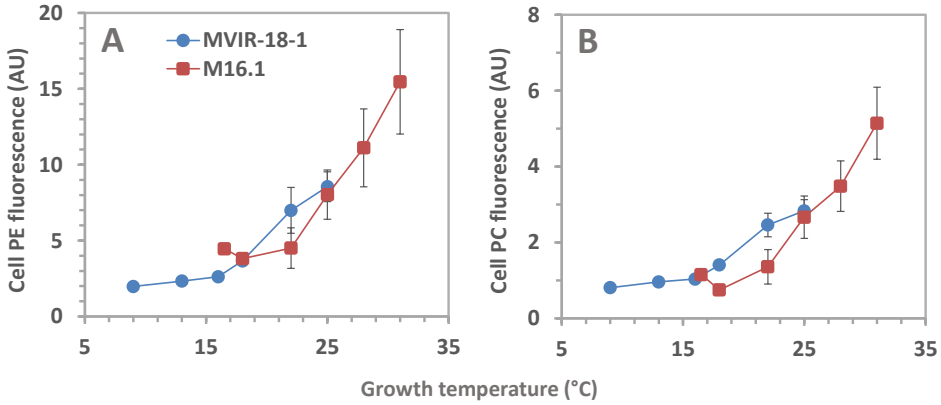

Figure S5: Variations of the cellular phycoerythrin (emission at 565-570 nm; **A**) and phycocyanin (emission at 651 nm; **B**) fluorescences, as measured by cell-normalized spectrofluorometry upon excitation at 530 nm.

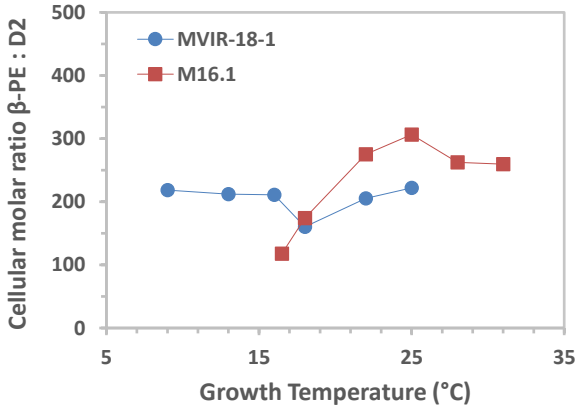

Figure S6: Variations of the cellular molar ratio of β-phycoerythrin (subunits CpeB and MpeB) to PsbD (core protein D2). This ratio is related to the phycobilisome to photosystem II molar ratio in the cells. Note that the values cited in the article are expressed in phycoerythrin hexamers per PsbD proteins.

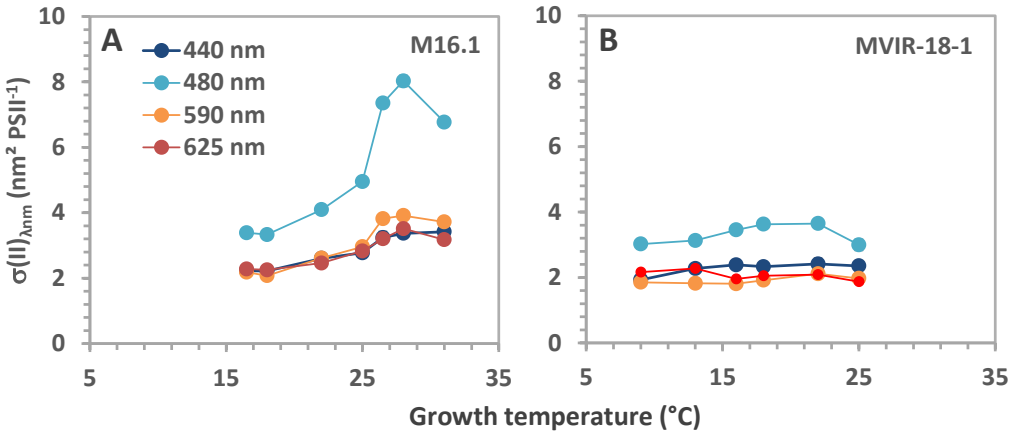

Figure S7: Variations of the photosystem II absorption cross-section at four different wavelengths as measured by recording O-I fast kinetics by pulse amplitude modulation fluorometry, in *Synechococcus* spp. M16.1 (**A**) and MVIR 18-1 (**B**).

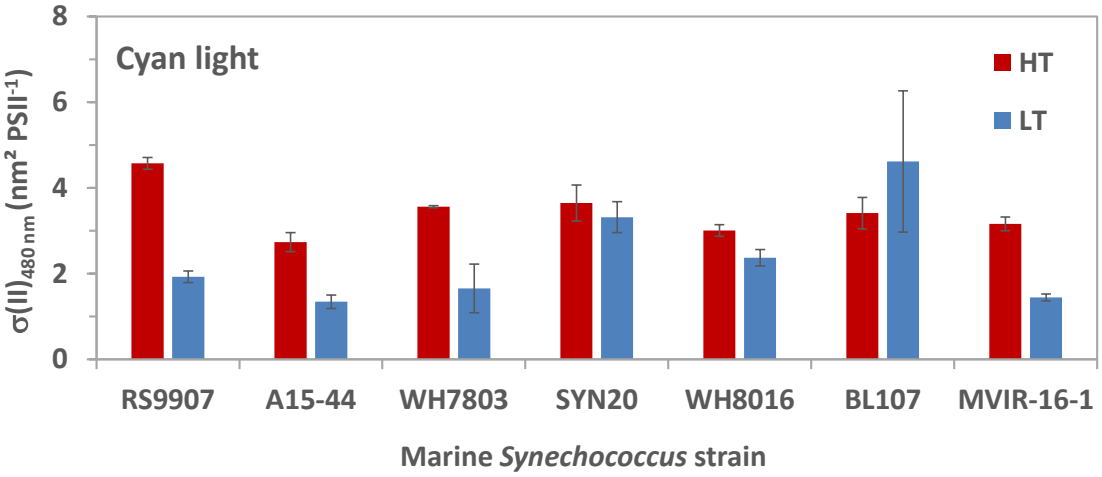

Figure S8: Variations of the photosystem II absorption cross-section at 480 nm in different temperature ecotypes of marine *Synechococcus* grown near their growth thermal limits. These results depend much of the phycourobilin content of the strains, which differ according to the pigment type. Warm adapted strains: RS9907 and A15-44 (Clade II), WH7803 (Clade V); Cold-adapted strains: SYN20 and WH8016 (Clade I), BL107 and MVIR-16-1 (Clade IV).

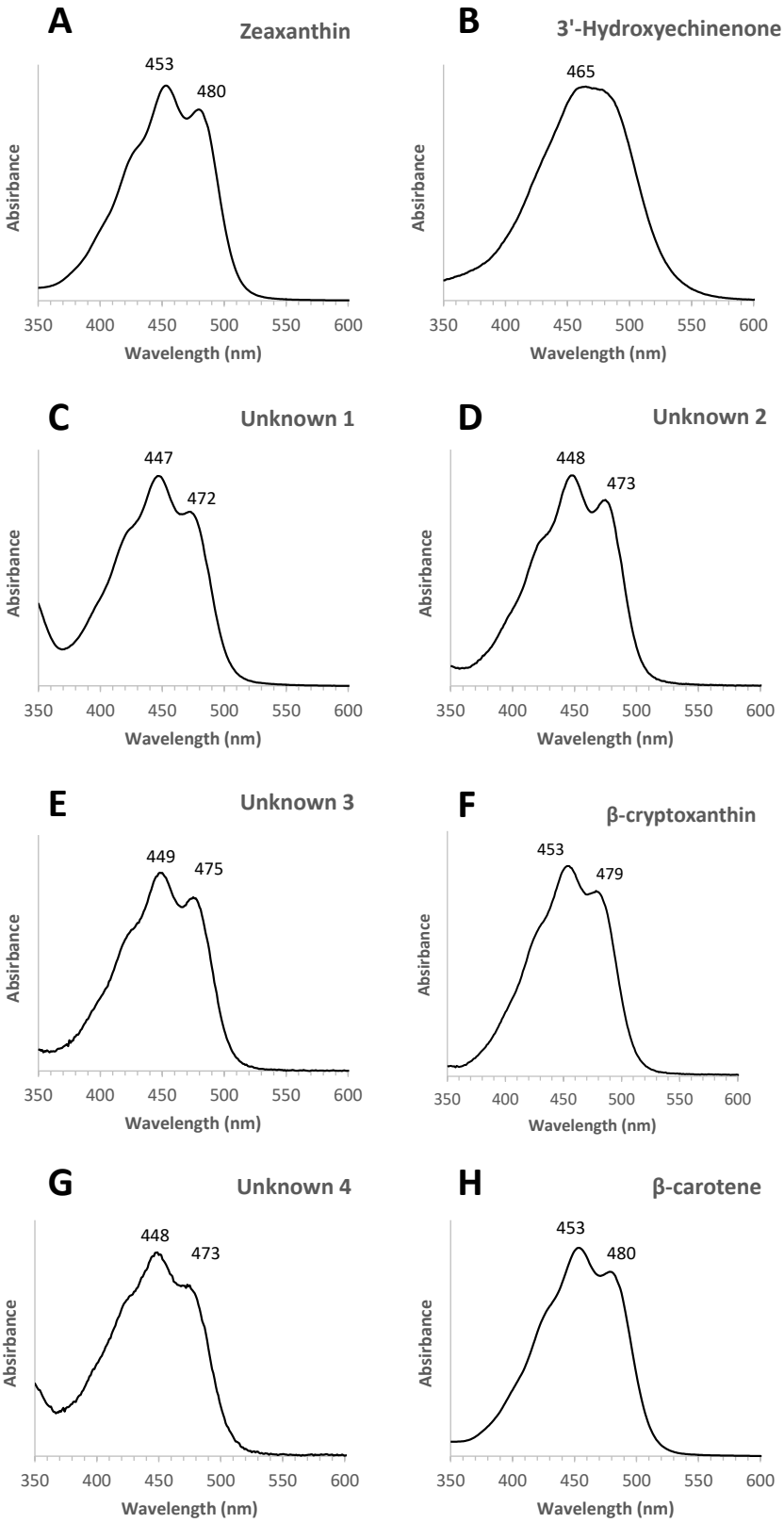

Figure S9: Absorbance spectra of the carotenoids detected in the marine *Synechococcus* strains MVIR-18-1 and M16.1, as measured by a photodiode array at their chromatographic retention time (Please see Fig. S11). Numbers indicate the wavelengths at which absorbance is maximal. Some of the unknown xanthophylls are probably zeaxanthin derivatives.

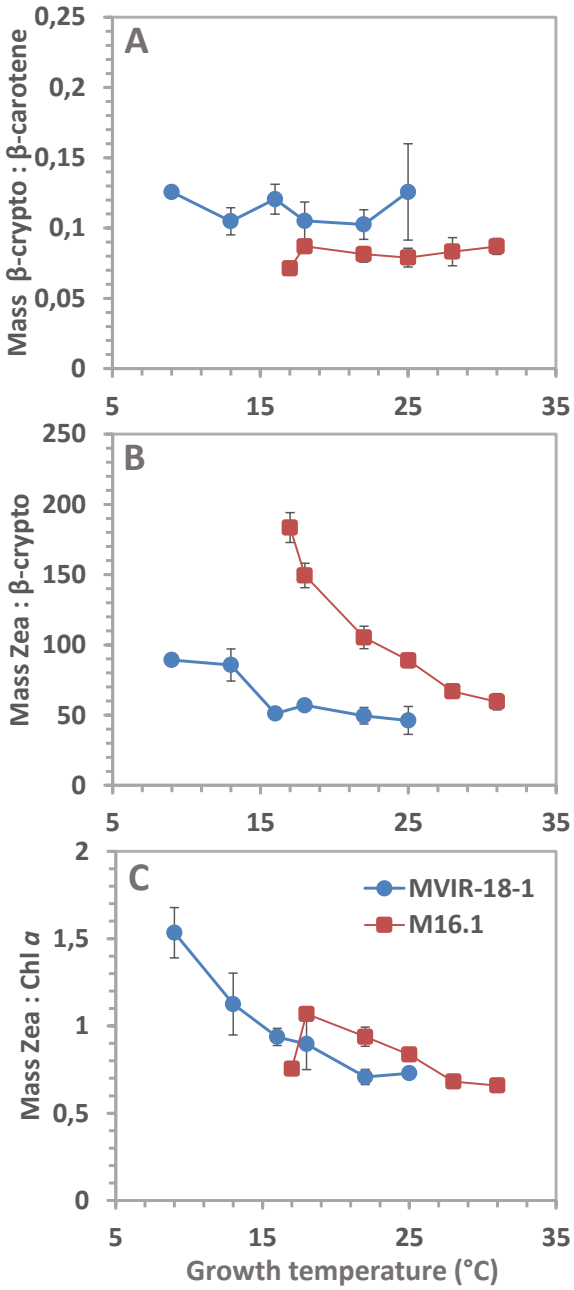

Figure S10: Variations of cellular mass pigment ratios of *Synechococcus* spp. M16.1 (red) and MVIR-18-1 (blue) grown over their thermal preferendum, as measured by high pressure liquid chromatography.

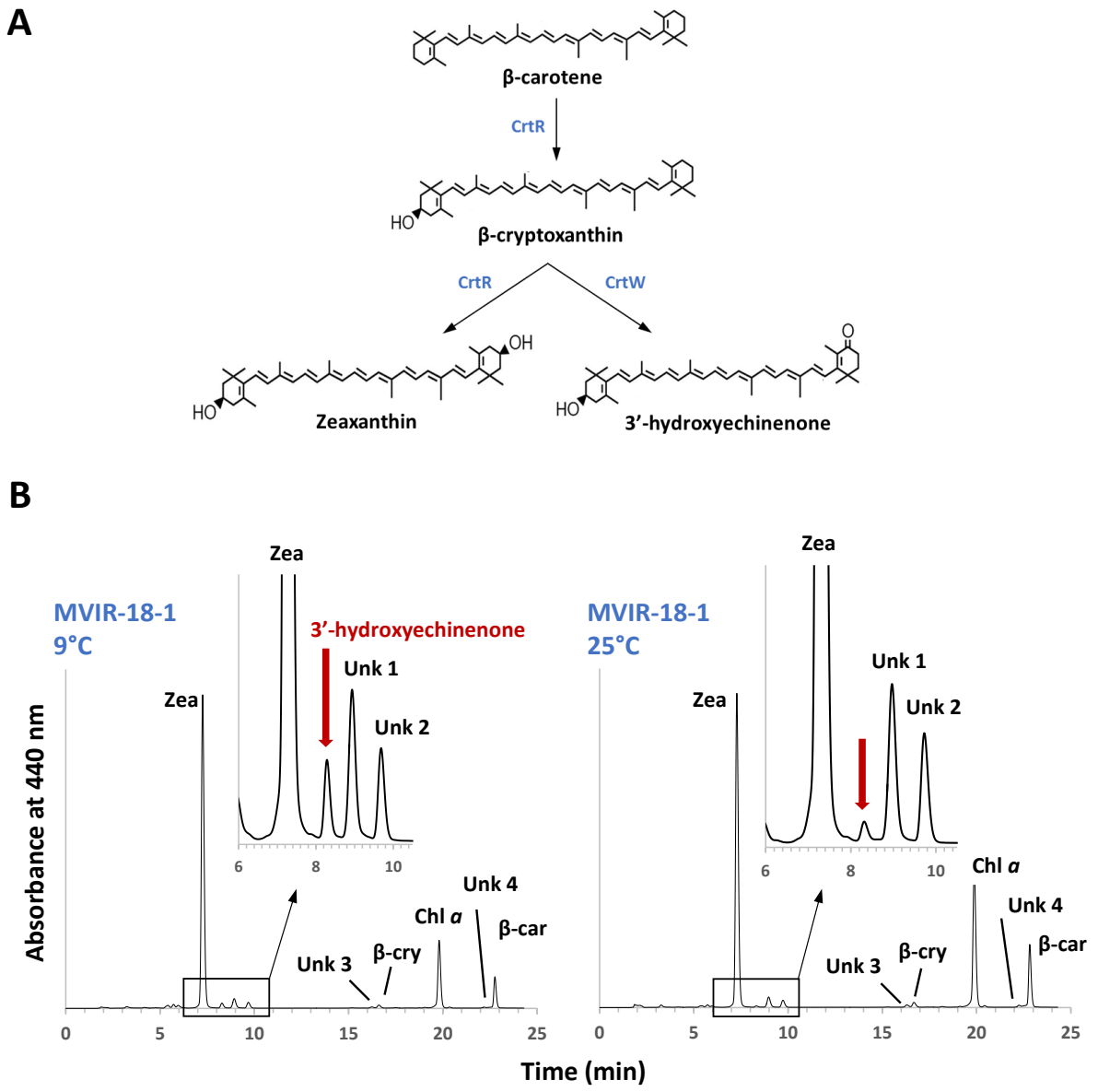

Figure S11: Possible biosynthesis pathway of zeaxanthin and 3'-hydroxyechinenone from β-carotene in marine *Synechococcus* (**A**). High pressure liquid chromatography analysis of membrane pigments showing the 3'-hydroxyechinenone peak (red arrow), in the subpolar *Synechococcus* sp. MVIR-18-1 grown at two extreme temperatures of the thermal *preferendum* (**B**). **β-car**: β-β-carotene; **β-cry**: β-β-cryptoxanthin; **Unk**: unknown xanthophyll; **Zea**: zeaxanthin.

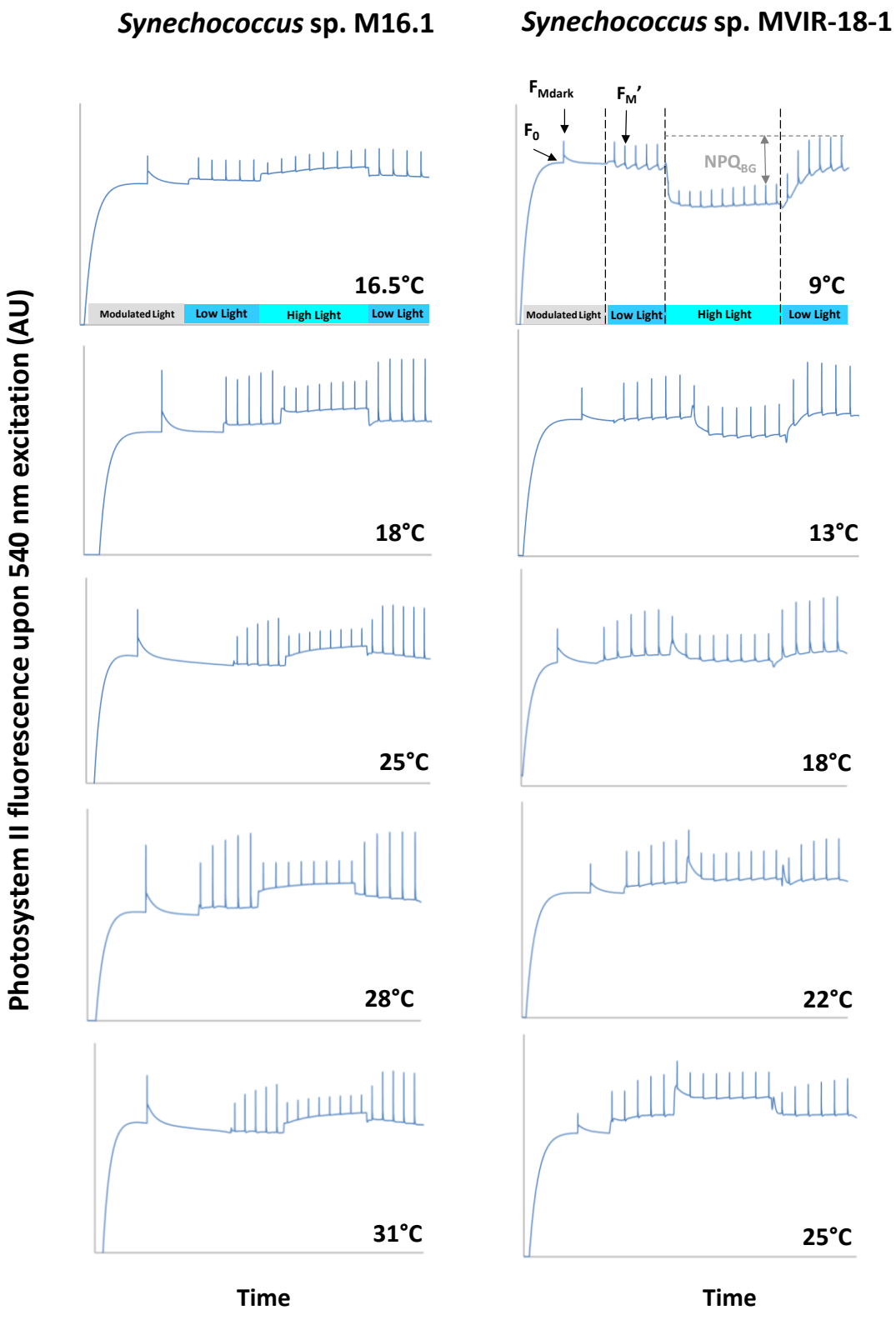

Figure S12: Examples of fluorescence traces recorded to study non photochemical quenching of fluorescence induced by high blue-green (480 nm) irradiance (NPQ_{BG}), in *Synechococcus* spp. M16.1 (left panel) and MVIR-18-1 (right panel), grown over their thermal *preferendum* . The different fluorescence levels are shown on MBIR-18-1 _9°C, the case showing maximal NPQ_{BG} in our experimental conditions. For a review see e.g. (9).

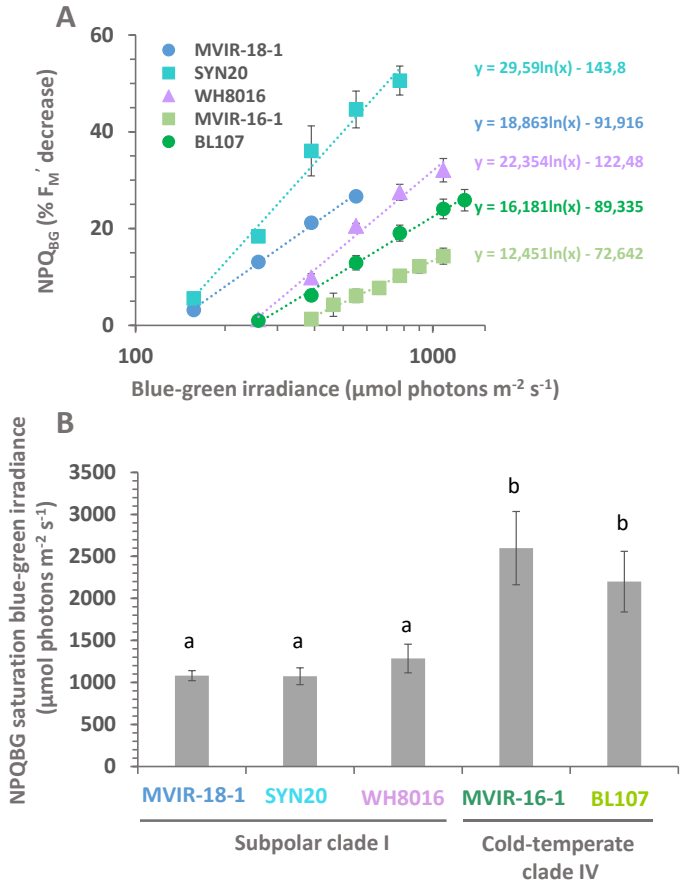

Figure S13: Ln-transformed irradiance response curves (**A**) and estimated saturation irradiances (**B**) of non-photochemical quenching of fluorescence induced by blue-green light (480 nm; NPQ_{BG}) for five cold-adapted strains of marine *Synechococcus* belonging to the cold-adapted clades I and IV (Kruskal-Wallis, *df*=3, *p*-value<0.05).

Section 2: Molecular characteristics of marine *Synechococcus* OCPs

Table S2: Accession numbers of sequences used to build the phylogenetic analysis of marine *Synechococcus* OCPs (cluster CK_00001790 in Cyanorak). Sequences from the Ocean Gene Atlas (OGA) were downloaded on the OGA website (10) and identified by their number in the Reference Gene Catalog database (OM-RGC; (11)).

	Sequence name	Origin	Clade	Accession
01	MVIR-18-1	MVIR-18-1 genome	I	CP047942
02	SYN20	SYN20 genome	I	CP047959
03	ROS8604	ROS8604 genome	I	CP047946
04	WH8016	WH8016 genome	I	AGIK00000000.1
05	CC9311	CC9311 genome	I	CP000435
06	WH8020	WH8020 genome	I	CP011941
07	PROS-9-1	PROS-9-1 genome	I	CP047961
08	UW179B	Lee et al. 2019	I	WP_115070113.1
09	MEDG-68	MEDG-68 metagenome	I	QOPS01000005
10	AG-686-F08	Metagenome	I	GCA_003210315.1
11	NP17	TARA Ocean	I	MBT66467.1
12	7340373	OGA, TARA Ocean	I	OM-RGC.v2.007340373
13	7307333	OGA, TARA Ocean	I	OM-RGC.v2.007307333
14	7454275	OGA, TARA Ocean	I	OM-RGC.v2.007454275
15	7325291	OGA, TARA Ocean	I	OM-RGC.v2.007325291
16	M16.1	M16.1 genome	II	CP047954

17	A15-44	A15-44 genome	II	CP047938
18	RS9907	RS9907 genome	II	CP047944
19	PROS-U-1	PROS-U-1 genome	II	CP047951
20	HB1133	HB1133 genome	II	SDBW00000000
21	UW86	Lee et al. 2019	II	WP_115161908.1
22	MED650	TARA Ocean	II	MAI95430.1
23	AG-673-B08	Metagenome	II	GCA_003209035.1
24	SAT82	TARA Ocean	II	MAX88342.1
25	UW69	Lee et al. 2019	II	WP_115021825.1
26	BS307-5m-G38	Cabello-Yeves et al. 2020	II	MBL6801897.1
27	7305616	OGA, TARA Ocean	II	OM-RGC.v2.007305616
28	7319027	OGA, TARA Ocean	II	OM-RGC.v2.007319027
29	7698709	OGA, TARA Ocean	II	OM-RGC.v2.007698709
30	BOUM118	BOUM118 genome	III	CP047947
31	WH8103	WH8103 genome	III	LN847356.1
32	WH8102	WH8102 genome	III	BX548020
33	RS9915	RS9915 genome	III	CP047934
34	A15-28	A15-28 genome	III	CP047931
35	A15-24	A15-24 genome	III	CP047960
36	A18-40	A18-40 genome	III	CP047956
37	A18-46.1	A18-46.1 genome	III	CP047955
38	MED-G133	MED-G133 metagenome	III	SHBS01000037
39	YX04-3	Zheng et al. 2020	III	RNC93067.1
40	7305562	OGA, TARA Ocean	III	OM-RGC.v2.007305562
41	7306351	OGA, TARA Ocean	III	OM-RGC.v2.007306351
42	BL107	BL107 genome	IV	AATZ00000000
43	CC9902	CC9902 genome	IV	CP000097
44	MED-G69	MED-G69 metagenome	IV	RCL56366.1
45	AG-683-C23	Metagenome	IV	GCA_003208835.1
46	5897902	OGA, TARA Ocean	IV	OM-RGC.v2.005897902
47	7305455	OGA, TARA Ocean	IV	OM-RGC.v2.007305455
48	6955513	OGA, TARA Ocean	IV	OM-RGC.v2.006955513
49	7344225	OGA, TARA Ocean	IV	OM-RGC.v2.007344225
50	WH7803	WH7803 genome	V/VI	CT971583
51	WH7805	WH7805 genome	V/VI	AAOK00000000
52	BMK-MC-1	BMK-MC-1 genome	V/VI	CP047939
53	PROS-7-1	PROS-7-1 genome	V/VI	CP047945
54	MEDNS5	MEDNS5 genome	V/VI	CP047952
55	TMED90	TARA Ocean	V/VI	OUX72510.1
56	BS301-5m-G53	Cabello-Yeves et al. 2020	V/VI	MBL6742682.1
57	RS9917	RS9917 genome	VIII	AANP00000000
58	RS9909	RS9909 genome	VIII	CP047943
59	WH8101	WH8101 genome	VIII	CP047932
60	BS55D	BS55D genome	VIII	PHQT00000000
61	BS56D	BS56D genome	VIII	PHQU00000000
62	ARS1019	TARA Ocean	VIII	ASM269032v1
63	7312865	OGA, TARA Ocean	VIII	OM-RGC.v2.007312865
64	A15-127	A15-127 genome	WPC1	CP047948
65	KORDI-49	KORDI-49 genome	WPC1	CP006270.1
66	7306326	OGA, TARA Ocean	WPC1	OM-RGC.v2.007306326
67	7342442	OGA, TARA Ocean	WPC1	OM-RGC.v2.007342442
68	RCC307	RCC307 genome	5.3	CT978603
69	TMED185	TARA Ocean	5.3	OUW39040.1
70	7305569	OGA, TARA Ocean	5.3	OM-RGC.v2.007305569

Structural functionalities of marine OCPs

Hereafter we use the amino acid numeration of *Synechocystis* sp. PCC 6803 strain, in order to facilitate comparison with previous studies. In the inactive orange conformation, the two domains form a globular protein whose conformation is notably maintained by a salt bridge arginine (R155) - glutamate (E244) in the middle of the protein. The bridge is conserved in all marine *Synechococcus* OCPs, with the difference that the negative charge is brought by an aspartate (S244) residue. The residues tyrosine Y201 and tryptophan W288, tyrosine Y44 and tryptophan W101, respectively involved in H-bonds with the keto-group and in Pi interactions with the hydroxyl group of the xanthophyll, are also well conserved in marine OCPs. The active red conformation of freshwater OCPs is notably maintained by the residues glutamate E34, proline P126 and tyrosine Y129. They are all conserved in marine OCPs, except that E34 can be replaced by a smaller aspartate D34 residue only in strains of the subpolar *Synechococcus* clade I. This is interesting because mutating this residue in *Synechocystis* sp. PCC 6803 has been shown to have a direct impact on the fluorescence quenching efficiency of the red conformation (12). Are also conserved the arginine R155 residue involved in the fixation to the phycobilisome, the glutamate E174 and the arginine R185 allowing the conformation back conversion, and the aspartate residue D220 interacting with the fluorescence recovery protein, which catalyzes the OCP back conversion. The other residue shown to be involved in this interaction, the phenylalanine F299, is replaced by a tyrosine in all marine *Synechococcus* OCPs. This globally suggests that the global OCP photocycle mechanism is well conserved in marine *Synechococcus*.

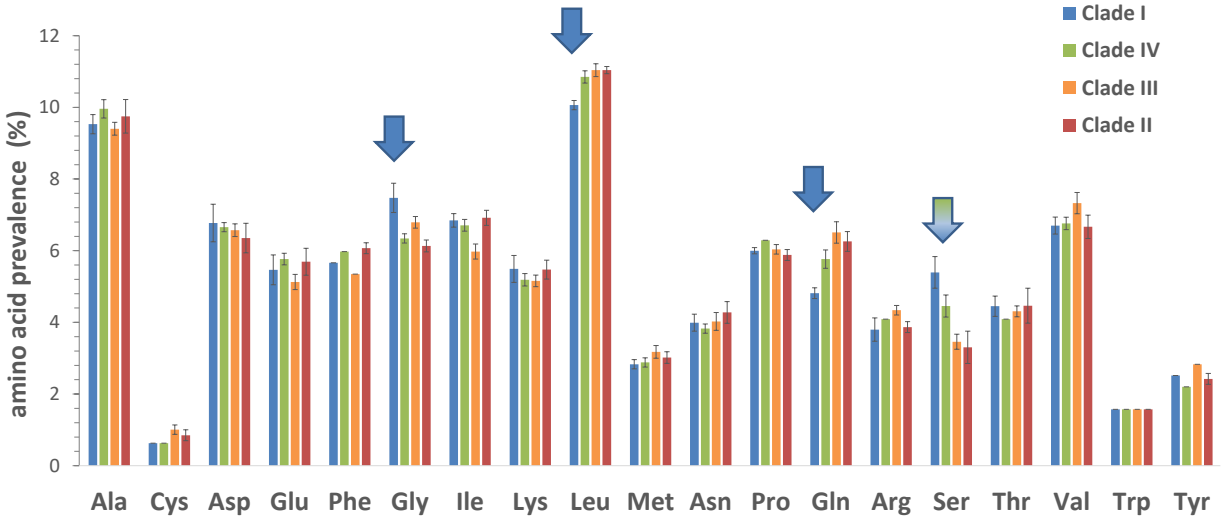

Figure S14: Relative composition in amino acid of the Orange Carotenoid Protein of marine *Synechococcus* thermotypes, including the subpolar clade I (11 sequences), the cold temperate clade IV (6 sequences), the warm temperate clade III (9 sequences) and the tropical clade II (11 sequences). There is no histidine in the protein. The arrows show the specific differences of clade I OCP sequences (blue) and of both clades I and IV (blue-green).

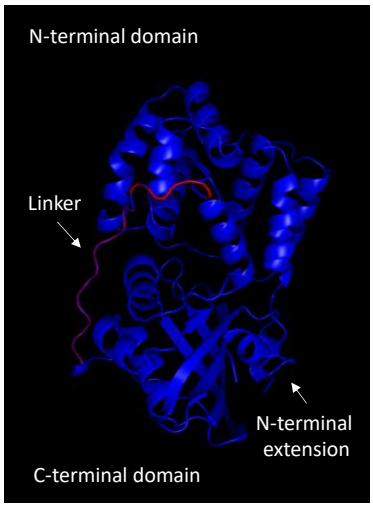

Figure S15: Differential structure model of the OCP of the subpolar MVIR-18-1 (blue) and the tropical M16.1 (red) *Synechococcus* strains. When the conformation is identical between the two superimposed protein structures, the MVIR-18-1 (blue) is shown. When there is a difference, both the subpolar and the tropical structures are shown. Note that the linker region appears to be the most different between the two OCPs.

Section 3: Metagenomics of *ocp* genes of marine *Synechococcus*

Table S3: Localization, seawater temperature and *petB* gene normalized counts of the sampling stations of the TARA expeditions (TARA Ocean and TARA Arctic) studied in this work.

TARA station #	Latitude	Longitude	Temperature (°C)	*petB* gene
4	36.6	-6.6	20.2	634.6
9	39.2	5.9	24.5	1322.3
23	42.2	17.7	17.2	759.6
25	39.4	19.4	18.3	2600.8
30	33.9	32.9	20.4	185.0
31	27.2	34.8	25.0	728.8
33	21.9	38.3	27.3	5215.8
34	18.4	39.9	27.6	3172.5
36	20.8	63.5	25.7	2578.9
38	19.0	64.5	26.3	3295.2
41	14.6	70.0	29.2	394.4
42	6.0	73.9	30.1	68.4
45	0.0	71.6	30.6	226.6
56	-15.3	43.3	27.3	153.0
57	-17.0	42.7	26.6	4483.6
62	-22.3	40.3	25.1	843.3
64	-29.5	38.0	22.2	820.6
65	-35.2	26.3	21.8	936.2
66	-34.9	17.9	15.0	125.1
67	-32.2	17.7	13.0	489.2
68	-31.0	4.7	16.9	2130.7
76	-20.9	-35.2	23.4	184.0
78	-30.1	-43.3	20.1	619.4
80	-40.7	-52.2	19.3	488.9
81	-44.5	-52.5	13.9	724.7
82	-47.2	-58.3	7.6	8.5
83	-54.4	-65.0	7.4	5.3
84	-60.2	-60.6	1.9	0
89	-57.7	-67.0	5.8	2.3
93	-34.1	-73.1	18.1	2381.0

123	-8.9	-140.5	26.6	1629.0
124	-9.2	-140.5	26.6	4412.9
140	7.4	-79.3	26.6	2529.8
141	9.8	-80.0	27.2	6831.4
145	39.2	-70.0	14.0	807.7
146	34.7	-71.3	19.3	887.3
148	31.7	-64.2	20.5	2034.5
149	34.1	-49.9	18.8	1088.2
150	35.9	-37.3	17.6	586.8
152	43.7	-16.8	14.3	1161.4
155	54.5	-16.8	11.1	538.8
210	61.5	-56.0	5.4	59.4

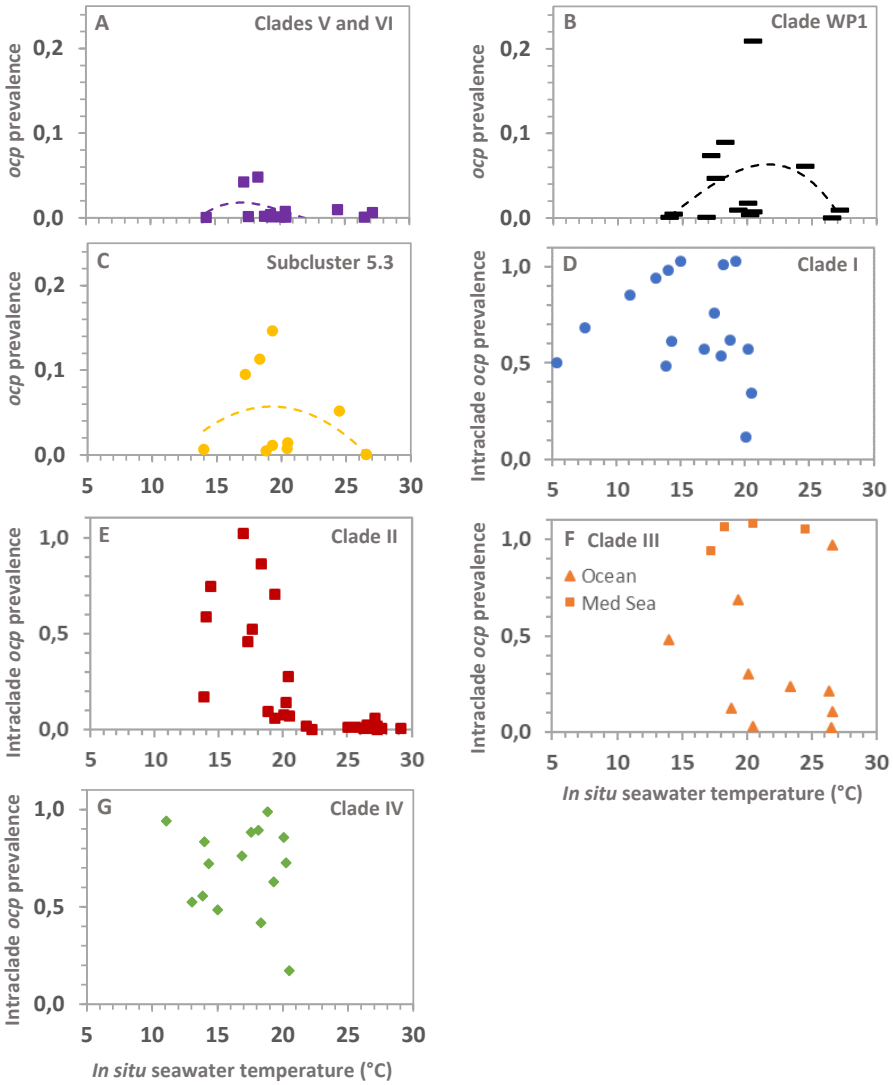

Figure S16: Prevalence of the *ocp* gene variants of the minor *Synechococcus* clades, function of seawater temperature (**A**, **B** and **C**). The values ≥ 0.1 are Mediterranean Sea stations. Intraclade prevalence of the *ocp* gene for th four major Synechococcus clades I (**D**), II (**E**), III (**F**) and IV (**G**)

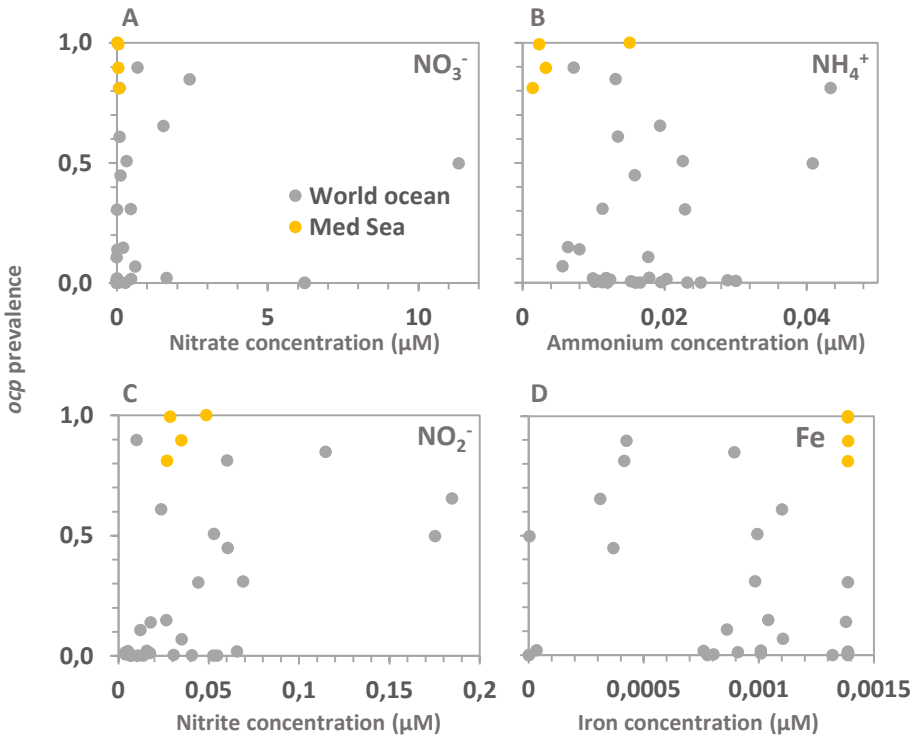

Figure S17: Prevalence of the *ocp* gene variants for all *Synechococcus* clades function of the concentration of nitrate (A), ammonium (B), nitrite (C) and iron (D) in seawater.

Section 4: Metabolic cost of thermal photophysiological acclimation

Dataset S1 (separate spreadsheet file): Study of the metabolic cost of thermoacclimation for major pigmented protein complexes, in the two *Synechococcus* temperature ecotypes M16.1 (tropical) and MVIR-18-1 (subpolar).

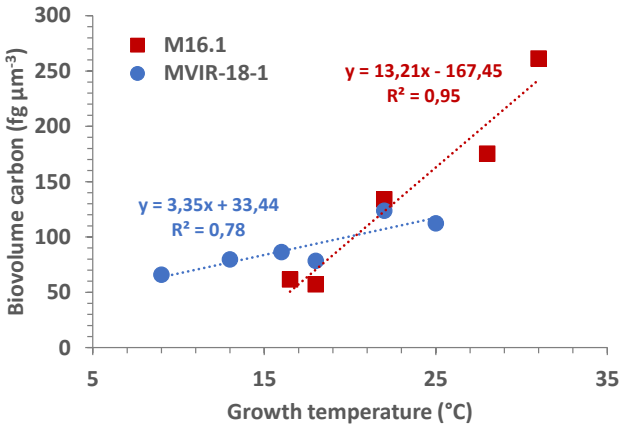

Figure S18: Allocation in carbon to photosynthetic pigmented complexes (phycobilisome, photosystem reaction centers and orange carotenoid protein) function of growth temperature, in *Synechococcus* spp. M16.1 (red) and MVIR-18-1 (blue).

References

1. S. Mazard, M. Ostrowski, F. Partensky, D. J. Scanlan, Multi-locus sequence analysis, taxonomic resolution and biogeography of marine *Synechococcus*. *Environ. Microbiol.* **14**, 372–386 (2012).
2. G. K. Farrant, *et al.*, Delineating ecologically significant taxonomic units from global patterns of marine picocyanobacteria. *Proc. Natl. Acad. Sci. U. S. A.* **113**, E3365–E3374 (2016).
3. H. Doré, *et al.*, Evolutionary Mechanisms of Long-Term Genome Diversification Associated With Niche Partitioning in Marine Picocyanobacteria. *Front. Microbiol.* **11**, 1–23 (2020).
4. J. Pittera, *et al.*, Connecting thermal physiology and latitudinal niche partitioning in marine *Synechococcus*. *ISME J.* **8**, 1–14 (2014).
5. C. Six, *et al.*, Diversity and evolution of phycobilisomes in marine *Synechococcus* spp.: a comparative genomics study. *Genome Biol.* **8**, R259 (2007).
6. F. Humily, *et al.*, A Gene Island with Two Possible Configurations Is Involved in Chromatic Acclimation in Marine *Synechococcus*. *PLoS One* **8**, e84459 (2013).
7. T. Platt, C. L. Gallegos, Modelling Primary Production. In: Falkowski P.G. (eds) Primary Productivity in the Sea. Environmental Science Research, vol 19. Springer, Boston, MA. https://doi.org/10.1007/978-1-4684-3890-1_19 (1980).
8. L. J. Ong, A. N. Glazer, Phycoerythrins of marine unicellular cyanobacteria: I. Bilin types and locations and energy transfer pathways in *Synechococcus* spp. phycoerythrins. *J. Biol. Chem.* **266**, 9515–9527 (1991).
9. D. Kirilovsky, Photoprotection in cyanobacteria: the orange carotenoid protein (OCP)-related non-photochemical-quenching mechanism. *Photosynth. Res.* **93**, 7–16 (2007).
10. E. Villar, T. Vannier, C. Vernette, M. Lescot, M. Cuenca, A. Alexandre, P. Bachelerie, T. Rosnet, E. Pelletier, S. Sunagawa, P. Hingamp. The Ocean Gene Atlas: exploring the biogeography of plankton genes online. Nucleic Acids Research doi: 10.1093/nar/gky376 (2018).
11. S. Sunagawa *et al.*, Structure and Function of the Global Ocean Microbiome. Science **348**, 1261359-1261359 (2015).
12. R. L. Leverenz, *et al.*, A 12 Å carotenoid translocation in a photoswitch associated with cyanobacterial photoprotection. Science **348**, 1463–1466 (2015).